

# Possible role of p53/Mieap-regulated mitochondrial quality control as a tumor suppressor in human breast cancer

Siqin Gaowa<sup>1</sup> | Manabu Futamura<sup>1</sup>  | Masayuki Tsuneki<sup>2</sup> | Hiroki Kamino<sup>2</sup> |  
Jesse Y. Tajima<sup>1</sup> | Ryutaro Mori<sup>1</sup> | Hirofumi Arakawa<sup>2</sup>  | Kazuhiro Yoshida<sup>1</sup>

<sup>1</sup>Department of Surgical Oncology, Graduate School of Medicine, Gifu University, Gifu, Japan

<sup>2</sup>Division of Cancer Biology, National Cancer Center Research Institute, Tokyo, Japan

## Correspondence

Manabu Futamura, Department of Surgical Oncology Gifu University, Graduate School of Medicine, Gifu, Japan.

Email: mfutamura@gifu-u.ac.jp

and

Hirofumi Arakawa, Division of Cancer Biology, National Cancer Center Research Institute, Tokyo, Japan.

Email: harakawa@ncc.go.jp

## Funding information

AMED, Grant/Award Number: 15ck0106006 h0002 (to HA); Ministry of Health, Labour and Welfare for the Practical Research for Innovative Cancer, Grant/Award Number: H26-practical-general-001 (to HA); KAKENHI, Grant/Award Number: 23659178 (to HA), 24240117 (to HA), 17K10542 (to MF) and 25670169 (to HA); The National Cancer Center Research and Development Fund, Grant/Award Number: 29-E-1 (to HA), 30-A-3 (to HA)

Mitochondria-eating protein (Mieap), encoded by a p53-target gene, plays an important role in mitochondrial quality control (MQC). Mieap has been reported to have a critical role in tumor suppression in colorectal cancer. Here, we investigated its role as a tumor suppressor in breast cancer. The enforced expression of exogenous Mieap in breast cancer cells induced caspase-dependent apoptosis, with activation of both caspase-3/7 and caspase-9. Immunohistochemistry revealed endogenous Mieap in the cytoplasm in 24/75 (32%) invasive ductal carcinomas (IDC), 15/27 (55.6%) cases of ductal carcinoma in situ (DCIS) and 16/18 (88.9%) fibroadenomas (FA) (IDC vs DCIS;  $P = 0.0389$ , DCIS vs FA;  $P = 0.0234$ , IDC vs FA;  $P < 0.0001$ ). In IDC, the *Mieap* promoter was methylated in 6/46 (13%) cases, whereas p53 was mutated in 6/46 (13%) cases. Therefore, the p53/Mieap-regulated MQC pathway was inactivated in 12/46 IDC (26.1%). Interestingly, all tumors derived from the 12 patients with *Mieap* promoter methylation or p53 mutations pathologically exhibited more aggressive and malignant breast cancer phenotypes. Impairment of p53/Mieap-regulated MQC pathway resulted in significantly shorter disease-free survival (DFS) ( $P = 0.021$ ), although p53 status is more prognostic in DFS than *Mieap* promoter methylation. These results indicate that p53/Mieap-regulated MQC has a critical role in tumor suppression in breast cancer, possibly in part through mitochondrial apoptotic pathway.

## KEYWORDS

apoptosis, breast cancer, caspase, Mieap, promoter methylation

## 1 | INTRODUCTION

Breast cancer is the most frequently diagnosed cancer and the leading cause of female cancer-associated death worldwide, accounting for 25% of all cancer cases and 15% of all cancer deaths among females.<sup>1,2</sup> Although the causes of breast cancer are not fully understood, some risk factors, including age, genetics, a family history of breast cancer and estrogen exposure, are known to affect its development.<sup>3,4</sup> Most hereditary breast cancers are

associated with alterations in either *BRCA1* or *BRCA2* (breast cancer susceptibility genes).<sup>5</sup> However, in sporadic breast cancers, the most important gene is *p53*, given that it is a tumor suppressor gene that is mutated in >50% of human cancers.<sup>6</sup> According to previous reports, *p53* is also mutated in approximately 20%-40% of breast cancers.<sup>7,8</sup> Recent data from The Cancer Genome Atlas revealed that 37% of breast cancer specimens had alterations in *p53* (72% in [human epidermal growth factor] HER2-rich and 80% in basal-like breast cancer cases), indicating that it is a critical

This is an open access article under the terms of the Creative Commons Attribution-NonCommercial License, which permits use, distribution and reproduction in any medium, provided the original work is properly cited and is not used for commercial purposes.

© 2018 The Authors. *Cancer Science* published by John Wiley & Sons Australia, Ltd on behalf of Japanese Cancer Association.

driver of tumor development even in breast cancer.<sup>9</sup> *p53* is clinically very important not only because of its high mutation rate but also because mutation is associated with more aggressive disease and worse overall survival.<sup>10</sup>

*p53* is a transcription factor that activates the expression of various downstream genes in response to DNA damage.<sup>11</sup> The central functions of this protein in tumor suppression are cell cycle arrest, apoptosis, DNA repair and anti-angiogenesis.<sup>12–16</sup> In particular, apoptosis is so important a function for *p53*-related tumor suppression that *p53* activates target genes, including *Bax*, *Noxa*, *Puma*, *Apaf-1* and *p53AIP1*, in response to DNA damage by radiation, UV and oxidative stress.<sup>11,13,17</sup> Although the mechanisms of apoptosis induced by DNA damage have been clarified, mitochondria are a pivotal organ for apoptosis, where these apoptosis-related proteins localize and play an important role in mitochondria through caspase activation.<sup>18</sup> Recently, mitochondrial quality control has been revealed to be a novel function of *p53*. This function is regulated by a novel *p53*-inducible protein called mitochondria-eating protein (*Mieap*).<sup>19,20</sup> *Mieap* plays an important role in mitochondrial quality control (MQC) by repairing or eliminating unhealthy mitochondria. *Mieap* carries out its repair function by inducing the accumulation of intramitochondrial lysosomal proteins to eliminate oxidized mitochondrial proteins in response to mitochondrial damage, in a process called *Mieap*-induced accumulation of lysosome-like organelles within mitochondria (MALM). This leads to a decrease in reactive oxygen species (ROS) generation and an increase in mitochondrial ATP synthesis. When MALM is inhibited, *Mieap* induces the formation of a vacuole-like structure known as the MIV. This engulfs the damaged mitochondria and results in the accumulation of lysosomes, leading to the degradation of unhealthy mitochondria.<sup>20</sup> Further *in vitro* study revealed that *BNIP3* and *NIX* co-localized with *Mieap* in mitochondria and reduced ROS. The physical interaction of *Mieap*, *BNIP3* and *NIX* at the mitochondrial outer membrane may play a critical role in the translocation of lysosomal proteins from the cytoplasm to the mitochondrial matrix.<sup>21</sup>

Although *Mieap* has been shown to be a key player in mitochondrial quality control, emerging evidence suggests that it also plays an important role in tumor suppression. In a mouse model, *Mieap*-deficient (adenomatous polyposis coli) *ApcMin/+* mice had a much shorter lifespan and increased numbers and sizes of intestinal tumors compared to those in *Mieap*-wild type *ApcMin/+* mice, suggesting that loss of *Mieap* increases ROS production in the intestinal mucosa and accelerates tumor progression.<sup>22</sup> Furthermore, *Mieap*-regulated mitochondrial quality control is frequently inactivated in human colorectal cancer by *Mieap* promoter methylation, *BNIP3* promoter methylation or *p53* mutation.<sup>23</sup> Considering that *Mieap* is a downstream target of *p53*, this novel mechanism for mitochondrial quality control is a new function of the *p53* tumor suppressor. These results strongly prompted us to speculate that *p53*/*Mieap*-regulated mitochondrial quality control might be involved in tumor suppression in human breast cancer. In this study, we investigated this role.

## 2 | MATERIALS AND METHODS

### 2.1 | Cell lines, cell culture, and drug

Breast cancer cell lines MCF-7 (luminal type), SK-BR-3 (HER2 type) and MDA-MB-231 (triple negative) were purchased from the ATCC (Manassas, VA, USA). All cell lines were grown in DMEM supplemented with 10% FBS (Sigma-Aldrich, St. Louis, MO, USA), antibiotics (Sigma-Aldrich) and non-essential amino acids in a humidified atmosphere of 5% CO<sub>2</sub> at 37°C. Etoposide was obtained from Sigma-Aldrich.

### 2.2 | Adenovirus

*Mieap*-expressing adenovirus (Ad-*Mieap*) was constructed as previously described.<sup>19,20</sup> As controls, we used Ad-EGFP, Ad-*BNIP3* and Ad- $\alpha$ 1-273 ( $\Delta$ 817), which express enhanced green fluorescent protein (EGFP), *BNIP3* and a *Mieap* deletion mutant lacking the C-terminal region (amino acids:1-273) of the *Mieap* protein (273 amino acids), respectively.<sup>20,21</sup> *BNIP3* is a BH3-only protein that belongs to the *Bcl-2* family and is suggested to induce apoptosis by inhibiting anti-apoptotic proteins.<sup>24</sup> Our group recently demonstrated that *BNIP3* is a co-factor of *Mieap* for MQC.<sup>21</sup>

### 2.3 | Fluorescence activated cell sorting analysis

We overexpressed *Mieap* using the constructed adenovirus in breast cancer cell lines. In addition, we treated these cells with etoposide (10  $\mu$ mol/L). MCF-7, SK-BR-3 and MDA-MB-231 cells were infected with the adenovirus at a moi of 30 and 60, respectively; cells were then trypsinized and washed with PBS. Subsequently, the cells were fixed in cold 70% ethanol at 4°C. Fixed cells were washed and then incubated for 30 minutes at 37°C with PBS containing 0.2 mg/mL RNase, and then incubated for a further 30 minutes at approximately 22°C with PBS containing 20  $\mu$ g/mL propidium iodide. Cells were analyzed using the EC800 Flow Cytometry Analyzer (Sony, Tokyo, Japan). For each analysis, 5000–20 000 cells were recorded, and the percentages of cells in different cell cycle phases (subG1, G1, S and G2/M) were determined using EC800 analysis software. The subG1 fraction was regarded as the apoptotic cell population.<sup>25</sup>

### 2.4 | Caspase activity assay

Breast cancer cell lines were treated using the same conditions as described previously herein. Caspase activities were measured as described previously.<sup>25</sup> The cell pellets were resuspended in cell lysis buffer (50 mmol/L HEPES, 100 mmol/L NaCl, 0.1% CHAPS, 1 mmol/L EDTA, 10% glycerol, 0.1% NP40, pH 7.4) for 15–30 minutes on ice. Total protein (10–30  $\mu$ g) was added to the reaction buffer (the same as the cell lysis buffer (except for the addition of 0.1% NP40) containing NAc-Asp-Glu-Val-Asp-pNA (Ac-DEVE-pNA, a substrate of caspase-3/7; Sigma-Aldrich), followed by

incubation for 1-2 hours at 37°C. The free pNA cleaved from its precursor was quantified using a spectrometer at 405 nm (Bio-Rad, Hercules, CA, USA). The Caspase-Glo 9 Assay reagent (Promega, Madison, MI, USA) was used as the substrate for activated caspase-9. An equal volume of cell lysate and caspase-Glo 9 reagent was added to each well, mixed, and incubated in the dark for 1 hour at room temperature. The resultant luminescence, which is proportional to caspase-9 activity, was measured using a luminometer (Bio-Rad). Absorbance was determined using an Envision 2104 multilabel reader (Perkin-Elmer, Waltham, MA, USA). Data were analyzed using Student's *t*-test. A *P*-value <0.05 was considered statistically significant.

## 2.5 | Western blotting

Caspase plays a central role in apoptosis, and the cleavage of poly ADP-ribose polymerase (PARP) facilitates cellular disassembly. Cleaved PARP is a marker of cells undergoing apoptosis.<sup>26</sup> Breast cancer cell lines were treated using the same conditions as those described previously herein. Cells were resuspended in radioimmunoprecipitation assay (RIPA) buffer (Sigma-Aldrich) with protease inhibitors for 15-30 minutes on ice. Protein (8 µg) was subjected to SDS-PAGE and then transferred to PVDF membranes. The membranes were blocked for 1 hour and then incubated with respective primary antibodies overnight at 4°C. The anti-Mieap antibody (rabbit, 1:1000) was prepared as described previously.<sup>19</sup> Anti-caspase-3 antibody (rabbit, 1:1000), anti-caspase-7 antibody (rabbit, 1:1000), anti-caspase-9 (rabbit, 1:1000), anti-cleaved PARP: poly (ADP-ribose) polymerase (rabbit, 1:2000), anti-Puma (rabbit, 1:1000), anti-Bax (rabbit, 1:1000), anti-Noxa (rabbit, 1:1000), anti-Bak (rabbit, 1:1000) (from Cell Signaling Technology, Danvers, MA, USA), anti-Apaf-1 (rat, 1:100), anti-caspase-8 (mouse, 1:200) (from Santa Cruz, Santa Cruz, CA, USA), anti-NIX (mouse, 1:250; Abnova, Taipei City, Taiwan) and anti-BNIP3 (mouse, 1:1000; Abcam, Cambridge, UK). The blots were stripped and re-probed with a β-actin antibody (1:5000; Cell Signaling Technology) to ensure equal protein loading. After washing, the membrane was incubated with secondary antibody (1:20000; ProteinTech, Chicago, IL, USA) for 1 hour at room temperature. The immunoreactive proteins were visualized and captured using the LAS-4000 system (Fujifilm, Tokyo, Japan).

## 2.6 | Immunohistochemistry

We examined the expression of Mieap *in vivo* using surgical specimens dissected at the Gifu University Hospital (invasive ductal carcinomas [IDC]: 75, ductal carcinoma in situ [DCIS]: 27, fibroadenomas [FA]: 18). Immunohistochemistry (IHC) was performed using Dako EnVision+ Dual Link System-HRP (Dako, Glostrup, Denmark). For antigen retrieval, sections were pretreated with 0.2% trypsin in 10 mmol/L tris-HCl (pH 7.6) containing 0.1% CaCl<sub>2</sub>, for 30 minutes at 37°C. Sections were incubated overnight at 4°C with the rabbit polyclonal anti-human Mieap antibody (diluted 1:200). Then, sections

were incubated with EnVision reagents for 1 hour at room temperature.<sup>22</sup> IHC evaluation was performed by experienced pathologists. When we started IHC for human cancer tissues *in vivo*, we repeated preliminary experiments for appropriate conditions using pre-immune serum. For subsequent runs, we did not use this due to its shortage. However, as we found endothelial cells and smooth muscle of blood vessels to be good positive controls, we show Mieap-expressing endothelial cells in Figure S1.

Informed consent was obtained from all patients who agreed to provide a surgical specimen. This study was approved by the central ethics committee of Gifu University.

## 2.7 | Methylation-specific PCR and p53 mutation search

Methylation-specific PCR was performed as described previously.<sup>19,23</sup> We used cryopreserved surgical specimens obtained from May 2011 to May 2012 at the Gifu University Hospital, most of which were also used for IHC, described previously. We extracted genomic DNA from 46 samples that were cryopreserved, among 75 IDC cases examined by immunohistochemistry, using DNeasy (Qiagen, Hilden, Germany). Bisulfite-treated genomic DNA was subjected to MSP. The MSP for *Mieap*, *NIX* and *BNIP3* promoters was carried out using specific primers under the following conditions: 1 cycle at 94°C for 5 minutes; 35 cycles at 94°C for 30 seconds, 57°C for 30 seconds and 72°C for 1 minute; and a final extension step at 72°C for 7 minutes. The *p53* mutation search was performed as described previously.<sup>23</sup> Genomic PCR was performed, followed by DNA sequence analysis.

## 2.8 | Statistical analysis

Immunohistochemistry for Mieap was analyzed using the  $\chi^2$ -test. Disease-free survival (DFS) was estimated using the Kaplan-Meier method, and comparisons between groups were performed using a 2-sided log-rank test. Results were considered significant at *P* < 0.05.

## 3 | RESULTS

### 3.1 | Mieap induces cell death in breast cancer cells

First, we investigated the expression level of Mieap protein in breast cancer cells (MCF-7, SK-BR-3 and MDA-MB-231) infected with Ad-Mieap (at a moi of 30-60). Twenty-four hours after adenovirus infection, exogenous Mieap protein was observed in each cell line by western blotting, and this was compared to that in control cells infected with EGFP-expressing adenovirus (Figure S2A). When Mieap was expressed in breast cancer cell lines, vacuole-like structures (Mieap-induced vacuoles [MIV]) were observed in the cytoplasm after 24 hours as previously reported (Figure S2B).<sup>20</sup>

MCF-7 cells were infected with Ad-Mieap at a moi of 5, 10, 20, 30 and 60. After 72 hours, we observed morphological changes microscopically and performed FACS analysis. MCF-7 cells were morphologically smaller, fragmented, and floated freely in the medium, and this phenomenon occurred in a dose-dependent manner (Figure 1A). FACS analysis demonstrated an increase in the subG1 fraction, suggesting nuclear DNA degradation in a moi-dependent manner (Figure 1B). We also examined the effect of Mieap on various breast cancer cells. After 48-72 hours of infection with Ad-Mieap (30-60 moi), each cell line was harvested for FACS analysis. Most cells were smaller and floating, particularly MCF-7 and SK-BR-3 cells, when compared to Ad-EGFP-infected cells (Figure 1C). The subG1 fractions were 56.94% for MCF-7 (30 moi, 72 hours) and 43.27% for SK-BR-3 (30 moi, 48 hours). In contrast, most MDA-MB-231 cells remained attached, with a subG1 fraction of 28.21% (60 moi, 72 hours; Figure 1D).

### 3.2 | Mieap-induced cell death is apoptosis

As a preliminary experiment, we treated 3 cell lines with etoposide. We found cleaved caspase-3/7/9 with activation of mitochondrial apoptotic factors particularly in SK-BR-3 and MDA-MB-231 (Figure S3).<sup>17,27</sup> To investigate the association between Mieap-induced cell death and caspases, we determined the expression levels and activation of caspase-3/7 and caspase-9 by western blotting and caspase activity assays. We found that SK-BR-3 was the most sensitive cell line to Mieap-induced cell death (Figure 1D). Forty-eight hours after Ad-Mieap infection (30 moi), not only caspase-3/7 but also caspase-9 was significantly elevated in SK-BR-3 cells (caspase-3/7:  $P = 0.000003$ , caspase-9:  $P = 0.0003$ ). In MCF-7 cells (Ad-Mieap: 30 moi), caspase-3/7 was significantly activated ( $P = 0.023$ ). However, in MDA-MB-231 cells (Ad-Mieap: 60 moi), no caspase activation was observed (Figure 2A). To confirm the activation

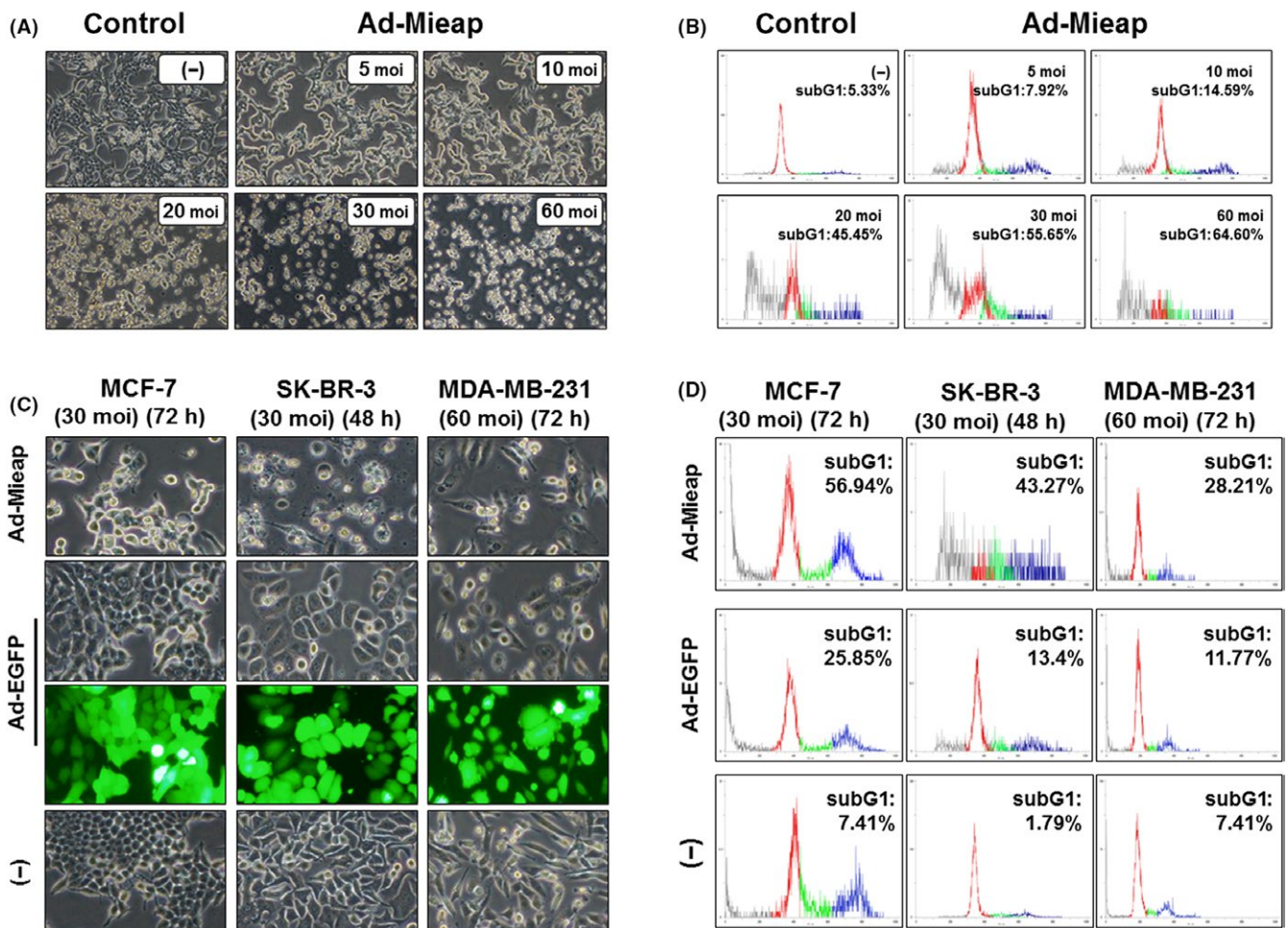


**FIGURE 1** Mieap-induced cell death in breast cancer cells occurs in a multiplicity of infection (moi)-dependent manner. A, After 72 h of Ad-Mieap infection, morphological changes were captured (100× magnification). Cell nuclei were fragmented, and the cell number was decreased in a moi-dependent manner. B, Adenovirus-infected cells (MCF-7) were collected and subjected to FACS analysis. Moi number and percentage of the subG1 fraction (apoptotic cells) are shown in the upper right of each diagram. C, Morphological changes in 3 breast cancer cell lines (MCF-7, SK-BR-3 and MDA-MB-231) 48-72 h after infection at a moi of 30-60 with Ad-Mieap. Ad-Mieap-infected cells were decreased in number and size. D, After incubation for the indicated time, cells were evaluated by flow cytometry. The subG1 fraction was elevated after Ad-Mieap infection. The subG1 fractions were 56.94% for MCF-7 (30 moi, 72 h) and 43.27% for SK-BR-3 (30 moi, 48 h). In contrast, most MDA-MB-231 cells remained attached, with a subG1 fraction of 28.21%

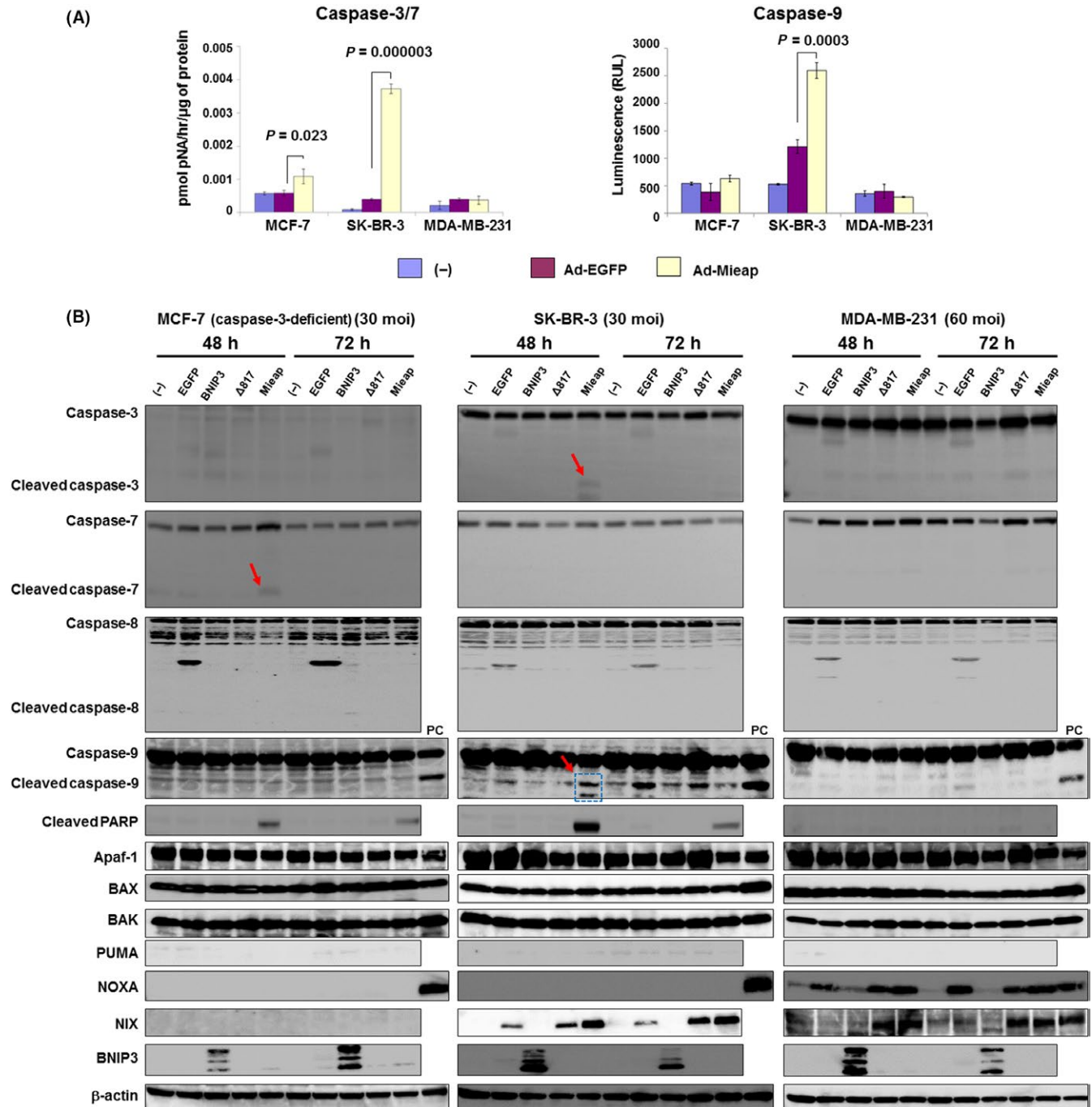


**FIGURE 2** Mieap activates mitochondrial apoptotic pathways in human breast cancer cells in a caspase-dependent manner. A, After 48 h (SK-BR-3) and 72 h (MCF-7, MDA-MB-231) treatments with adenovirus (30 multiplicity of infection (moi) for MCF-7 and SK-BR-3 and 60 moi for MDA-MB-231), caspase-3/7 (left) and caspase-9 (right) activities were measured. Caspases were significantly elevated in SK-BR-3 and MCF-7 cells but not in MDA-MB-231 cells. B, Western blotting data for cleaved caspase-3/7 (red arrows) and cleaved poly (ADP-ribose) polymerase are indicated. Cell lysates from 3 breast cancer cell lines were harvested under the indicated conditions (48-72 h, 30-60 moi). Caspase-3-deficient MCF-7 cells showed cleavage of caspase 7. No cleaved caspase-8 was detected in any of the cells and caspase-9 was cleaved in SK-BR-3 cells (arrow and dotted box). No mitochondria-associated apoptotic factors were altered in MCF-7 cells. In SK-BR-3 cells, NIX was elevated, resulting in caspase-9 activation. Despite activation of both NOXA and NIX, caspases including caspase-9 were not activated in MDA-MB-231 cells. Based on these data, Mieap can activate the mitochondria apoptotic pathway. However, the occurrence of Mieap-induced cell death depends on caspase activation. PC indicates positive control. No infection (-), Ad-EGFP, Ad-BNIP3 and Ad-Δ817 (deletion mutant [273 amino acids] of Mieap) were used as negative controls

of caspases, we performed western blotting for caspase-3/7 and PARP. In SK-BR-3 cells, caspase-3 was cleaved 48 hours after Ad-Mieap infection. In MCF-7 cells, caspase-7, but not caspase-3, was

cleaved under the same conditions because caspase-3 is deficient in MCF-7 cells.<sup>28</sup> Cleaved PARP, which is produced through cleavage by activated caspases,<sup>29</sup> was detected 48-72 hours after Ad-Mieap

infection in both cell lines. These results indicate that activation of caspase is a major cause of Mieap-induced cell death. In contrast, in MDA-MB-231 cells, we could detect neither the activation of these caspases nor cleaved PARP, indicating that MDA-MB-231 cells might be resistant to Mieap-induced cell death (Figure 2B).

Interestingly, in SK-BR-3 cells, cleaved caspase-9/3 was detected after 48 hours of Ad-Mieap treatment and was associated with NIX elevation. Although in MDA-MB-231 cells NOXA and NIX were elevated, neither caspases nor PARP was cleaved. In MCF-7 cells, which are caspase-3-deficient cells, only caspase-7 was cleaved, with no upregulation of mitochondrial apoptotic factors. We further investigated the expression of BNIP3/NIX in each cell line. Both proteins were not expressed in steady-state conditions; however, NIX was elevated in SK-BR-3 and MDA-MB-231 after Ad-Mieap infection. BNIP3 was not expressed irrespective of enforced Mieap expression. These results indicated that Mieap is involved in the mitochondrial apoptotic pathway in a caspase-dependent manner. Based on these results, we concluded that Mieap-induced cell death is apoptosis and that it is mediated by the mitochondrial apoptotic pathway.

### 3.3 | Mieap expression is downregulated in tumors from breast cancer patients with an aggressive and malignant phenotype

We next performed IHC using surgical specimens obtained from 120 patients (IDC: 75, DCIS: 27, and FA: 18) to examine the expression of Mieap in vivo. Mieap was detected in the cytoplasm, and representative cases (both positive and negative cases, respectively) are shown in Figure 3. Mieap was positive in 32% (24/75) of IDC, 55.6% (15/27) of DCIS and 88.9% (16/18) of FA. Its expression was also significantly higher in FA compared to that in DCIS ( $P = 0.0234$ ), in DCIS compared to that in IDC ( $P = 0.0389$ ), and in FA compared to that in IDC ( $P < 0.0001$ ), indicating that its expression decreases with malignant potential (Table 1).

### 3.4 | The p53/Mieap-regulated mitochondrial quality control pathway is genetically and epigenetically inactivated in aggressive and malignant breast cancer

To investigate inactivation of the p53/Mieap-regulated MQC pathway, we performed MSP for *Mieap*, *NIX* and *BNIP3* promoters, as well as a *p53* mutation search, because *NIX* and *BNIP3* have been shown to be co-factors for MQC.<sup>21</sup> We investigated 46 IDC, which had been stored as frozen tissue for DNA extraction. MSP revealed methylation of the *Mieap* promoter in 6 of 46 IDC (13%). However, there was no methylation of the *NIX* or *BNIP3* promoters (Figure 4). Genetic alterations of *p53* were found in 6 of 46 IDC (13%). The p53/Mieap-regulated MQC pathway was inactivated in 12 of 46 IDC (26.1%; Table 2). Of 12 cases, 6 with methylated *Mieap* promoter were luminal B and the other 6 with mutant *p53* were triple negative as follows: 4, HER2-rich; 1, luminal B; 1, whose subtypes were clinically more aggressive and malignant phenotypes in breast cancer (Table 3).<sup>30,31</sup>

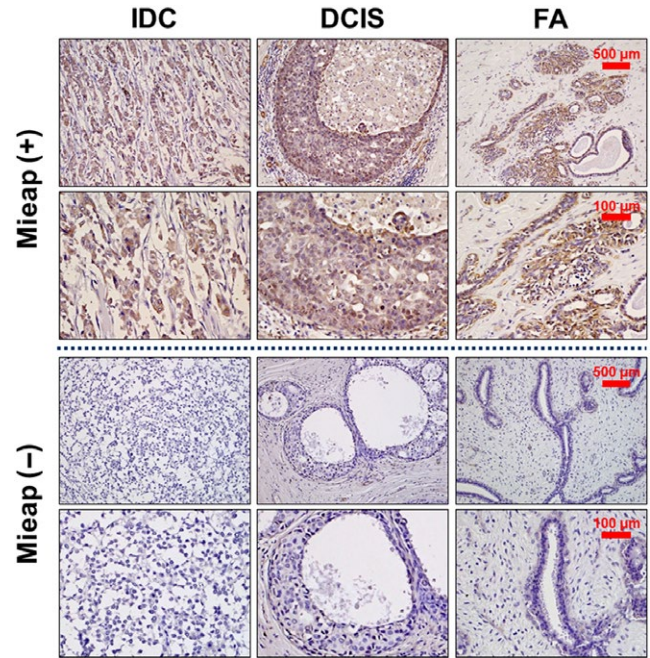


**FIGURE 3** Immunohistochemistry for Mieap in breast tumors in vivo. Immunohistochemical staining of Mieap in tissue specimens obtained from patients with invasive ductal carcinomas (IDC), ductal carcinoma in situ (DCIS) and fibroadenomas (FA). Representative cases (Mieap-positive [+], Mieap-negative [-]) are indicated. Mieap is expressed in the cytoplasm. The scale bars represent 500  $\mu\text{m}$  (upper row) and 100  $\mu\text{m}$  (lower row) photomicrographs

Interestingly, the group with inactivation of the p53/Mieap-regulated MQC pathway showed shorter DFS than that without these genetic alterations ( $P = 0.021$ , Figure 5). Four of six recurrent cases showed inactivation in the p53/Mieap-regulated MQC pathway. Of 46 cases, we separately showed DFS curves for individuals with or without *Mieap* promoter methylation or those with or without *p53* alterations (Figure S4). As shown in Figure S4A, there was no significant difference between those with *Mieap* promoter methylation ( $n = 6$ ) and those without ( $n = 40$ ). Six cases with a methylated *Mieap* promoter showed no expression of Mieap by IHC. However, as shown in Figure S4B, there was a significant difference between those with *p53* mutations ( $n = 6$ ) and those without ( $n = 40$ ;  $P = 0.00035$ ). Considering *p53*-mutated cases, 4 of 5 revealed no Mieap expression. Mieap expression was completely undetectable in 10 of 11 cases with either methylated *Mieap* promoter or *p53* alterations. In addition, as shown in Figure S4C, among 75 IDC evaluated by IHC (in Figure 3), there were no significant differences between 24 Mieap-positive IDC cases and 51 Mieap-negative cases. These results suggest that Mieap might not be prognostic, at least to the same extent as *p53*. Based on the previous reports that Mieap expression is regulated by either *p53* status or methylation of *Mieap*, *BNIP3* and *NIX* promoters, we suggest that it is important to evaluate MQC based on these factors (i.e. MQC pathway through p53 and BNIP3/NIX to Mieap).

**TABLE 1** Immunohistochemistry for Mieap in vivo using human breast cancer tissues

	Mieap (+)	Mieap (-)	Positive rate (%)		
Invasive ductal carcinoma (IDC)	24	51	32	p=0.0389	p<0.0001
Ductal carcinoma in situ (DCIS)	15	12	55.6		
Fibroadenoma (FA)	16	2	88.9		

Paraffin-embedded specimens obtained from surgery (invasive ductal carcinomas [IDC]: 75, ductal carcinoma in situ [DCIS]: 27, and fibroadenomas [FA]: 18) were examined using an anti-human-Mieap antibody. Positive rates in IDC, DCIS and FA were 32%, 55.6% and 88.9%, respectively. The positive rate for Mieap in IDC was significantly lower than that in DCIS ( $P = 0.0389$ ) and FA ( $P < 0.0001$ ).

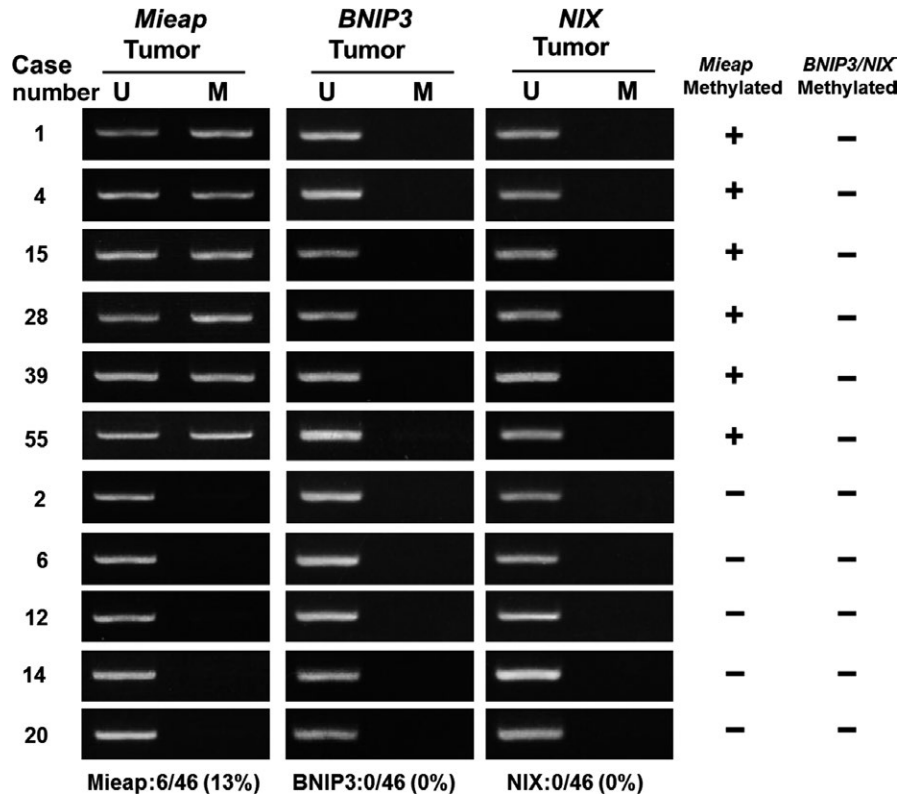


**FIGURE 4** Methylation-specific PCR (MSP) and breast cancer clinical outcome based on inactivation of Mieap-regulated mitochondrial quality control (MQC). MSP analysis of the *Mieap*, *NIX* and *BNIP3* promoters. Genomic DNA was extracted from surgically dissected invasive breast cancer and then treated with bisulfite treatment and subjected to MSP for *Mieap/NIX/BNIP3* promoters. The results of MSP from 11 representative cases are shown. *Mieap* promoter methylation was detected in 6 cases. However, no samples showed *NIX/BNIP3* methylation. M, methylated; U, unmethylated

## 4 | DISCUSSION

According to a previous report, we demonstrated the physiological functions related to MQC, which were classified mainly into 2 mechanisms. One is referred to as MALM, whereas the other is MIV, which occurs when salvage of the damaged mitochondria appears to be impossible for recovery and survival.<sup>20</sup> These mechanisms might be used depending on the degree of mitochondrial damage. In this study, we focused on the MIV, followed by Mieap-induced cell death, and found strong evidence supporting the role of Mieap in breast cancer tumor suppression.

First, Mieap induced caspase-dependent apoptosis in breast cancer cells. We infected adenoviruses at a moi of 30-60 into each cell (for MIV), for which Ad-Mieap mois were 5-10-fold greater compared to that for MALM. This Mieap-induced apoptosis was likely

consistent with the mitochondrial intrinsic pathway because Mieap activated caspase-9/3 as observed in SK-BR-3 cells. However, given that MCF-7 cells are known to be a caspase-3-deficient cell line,<sup>28</sup> caspase-7 was suggested to function instead, as Ac-DEVE-pNA is a substrate for both caspase-3 and caspase-7. Lakhani et al<sup>26</sup> report that both caspase-3 and caspase-7 regulate mitochondrial events in the apoptotic pathway. These results suggest that apoptosis induced by Mieap occurs via a caspase-dependent intrinsic pathway through the mitochondria. Through our experiments using 3 cell lines, we identified at least 3 patterns against Mieap: (i) good response: in SK-BR-3 cells, Mieap activates apoptotic factors in the mitochondria in a caspase (9/3)-dependent manner; (ii) fair response: in MCF7 cells, Mieap activates apoptotic factors in mitochondria; however, cells do not undergo enough apoptosis, exhibiting activation of caspase-7, but

**TABLE 2** Association between regulatory factors of Mieap expression and subtypes

Case	Mieap methylated	NIX methylated	BNIP3 methylated	p53 mutation	Mieap expression	Subtype
1	+	-	-	-	-	Luminal B
4	+	-	-	-	-	Luminal B
15	+	-	-	-	-	Luminal B
28	+	-	-	-	-	Luminal B
39	+	-	-	-	-	Luminal B
55	+	-	-	-	-	Luminal B
10	-	-	-	Deletion in exon 4	-	Triple negative
32	-	-	-	Deletion in exon 4	-	Triple negative
35	-	-	-	Deletion in exon 7	-	Triple negative
42	-	-	-	TGC→TGG(176C→W)	+	Triple negative
52	-	-	-	CGT→TGT (273R→C)	-	Luminal B
56	-	-	-	GAC→CAC (281D→H)	NE	HER2
13	-	-	-	-	+	Luminal A
33	-	-	-	-	+	Triple negative
40	-	-	-	-	+	Luminal B
44	-	-	-	-	+	Luminal A
49	-	-	-	-	+	Luminal B
50	-	-	-	-	+	Luminal B
2	-	-	-	-	-	Luminal A
6	-	-	-	-	-	HER2
11	-	-	-	-	-	Luminal/HER2
12	-	-	-	-	NE	Luminal/HER2
16	-	-	-	-	-	Luminal A
17	-	-	-	-	-	Luminal A
18	-	-	-	-	-	Luminal B
19	-	-	-	-	-	Luminal A
20	-	-	-	-	-	Luminal A
22	-	-	-	-	-	Luminal A
23	-	-	-	-	-	Luminal B
24	-	-	-	-	-	Luminal A
25	-	-	-	-	-	Luminal A
26	-	-	-	-	-	Luminal B
27	-	-	-	-	-	Luminal B
29	-	-	-	-	NE	Luminal B
30	-	-	-	-	-	Luminal A
31	-	-	-	-	-	Luminal A
34	-	-	-	-	NE	Luminal A
37	-	-	-	-	-	Triple negative
38	-	-	-	-	-	Luminal A
41	-	-	-	-	-	Luminal B
43	-	-	-	-	-	Triple negative
46	-	-	-	-	-	Luminal A
47	-	-	-	-	-	Luminal A
48	-	-	-	-	NE	Luminal A
53	-	-	-	-	-	Luminal B

(Continues)

**TABLE 2** (Continued)

Case	Mieap methylated	NIX methylated	BNIP3 methylated	p53 mutation	Mieap expression	Subtype
54	-	-	-	-	-	Luminal A
	6/46 (13%)	0/46 (0%)	0/46 (0%)	6/46 (13%)	7/41 (17%)	

NE, not examined.

Results of MSP for *Mieap*/*NIX*/*BNIP3* promoters and *p53*-mutation search (exons 4-8) are summarized. Methylation of the *Mieap* promoter was positive in 6/46 (13%) cases, whereas *NIX*/*BNIP3* promoters were negative. Genetic alterations in *p53* were detected in 6/46 (13%) cases. Finally, inactivation of the *p53*/*Mieap*/*NIX*/*BNIP3*-regulated mitochondrial quality control (MQC) pathway was observed in 12/46 (26.1%) cases. These cases were aggressive phenotypes such as Luminal B, triple negative and HER2-enriched. Among them, ten cases of 11 subjected to IHC lost *Mieap* expression.

**TABLE 3** Summary of clinicopathological parameters in human breast cancers

Case	Age	Gender	Subtype	TN	Stage	Recurrence	Histopathological diagnosis
1	58	Female	Luminal B	T4bN1	IIIB	-	Scirrhous carcinoma
4	46	Female	Luminal B	T2N0	IIA	-	Scirrhous carcinoma
15	76	Female	Luminal B	T1N0	I	-	Invasive lobular carcinoma
28	48	Female	Luminal B	T2N1	IIB	+	Solid-tubular carcinoma
39	51	Female	Luminal B	T3N1	IIIA	-	Scirrhous carcinoma
55	72	Female	Luminal B	T2N0	IIA	-	Scirrhous carcinoma
2	74	Female	Luminal A	T2N0	IIA	-	Solid-tubular carcinoma
6	36	Female	HER2	T2N1	IIB	+	Scirrhous carcinoma
10	69	Female	Triple negative	T1N1	IIA	-	Solid-tubular carcinoma
11	45	Female	Luminal/HER2	T1N0	I	-	Scirrhous carcinoma
12	75	Female	Luminal/HER2	T1N2	IIB	-	Solid-tubular carcinoma
13	72	Female	Luminal A	T1N0	I	-	Scirrhous carcinoma
16	51	Female	Luminal A	T1N1	IIA	-	Papillotubular carcinoma
17	60	Female	Luminal A	T2N0	IIA	-	Papillotubular carcinoma
18	43	Female	Luminal B	T2N0	IIA	-	Papillotubular carcinoma
19	66	Female	Luminal A	T1N1	IIA	-	Scirrhous carcinoma
20	79	Female	Luminal A	T1N0	I	-	Solid-tubular carcinoma
22	58	Female	Luminal A	T1N1	IIA	-	Scirrhous carcinoma
23	84	Female	Luminal B	T1N0	I	-	Scirrhous carcinoma
24	62	Female	Luminal A	T2N0	IIA	-	Scirrhous carcinoma
25	63	Female	Luminal A	T2N0	IIA	+	Scirrhous carcinoma
26	49	Female	Luminal B	T1N1	IIA	-	Solid-tubular carcinoma
27	48	Female	Luminal B	T2N0	IIA	-	Scirrhous carcinoma
29	57	Female	Luminal B	T2N1	IIB	-	Mucinous carcinoma
30	61	Female	Luminal A	T2N1	IIB	-	Scirrhous carcinoma
31	64	Female	Luminal A	T2N1	IIB	-	Scirrhous carcinoma
32	52	Female	Triple negative	T2N0	IIA	-	Solid-tubular carcinoma
33	69	Female	Triple negative	T2N0	IIA	-	Papillotubular carcinoma
34	51	Female	Luminal A	T1N0	I	-	Papillotubular carcinoma
35	46	Female	Triple negative	T2N0	IIA	+	Solid-tubular carcinoma
37	62	Female	Triple negative	T1N0	I	-	Scirrhous carcinoma
38	53	Female	Luminal A	T1N0	I	-	Papillotubular carcinoma
40	42	Female	Luminal B	T2N1	IIB	-	Papillotubular carcinoma
41	68	Female	Luminal B	T1N0	I	-	Solid-tubular carcinoma
42	57	Female	Triple negative	T2N1	IIB	+	Scirrhous carcinoma
43	79	Female	Triple negative	T2N0	IIA	-	Papillotubular carcinoma

(Continues)

TABLE 3 (Continued)

Case	Age	Gender	Subtype	TN	Stage	Recurrence	Histopathological diagnosis
44	51	Female	Luminal A	T1N0	I	-	Papillotubular carcinoma
46	64	Female	Luminal A	T1N0	I	-	Papillotubular carcinoma
47	63	Female	Luminal A	T1N0	I	-	Scirrhous carcinoma
48	73	Female	Luminal A	T1N0	I	-	Papillotubular carcinoma
49	33	Female	Luminal B	T1N0	I	-	Scirrhous carcinoma
50	58	Female	Luminal B	T2N0	IIA	-	Solid-tubular carcinoma
52	74	Female	Luminal B	T4bN1	IIIB	+	Scirrhous carcinoma
53	46	Female	Luminal B	T2N0	IIA	-	Papillotubular carcinoma
54	70	Female	Luminal A	T1N0	I	-	Papillotubular carcinoma
56	68	Female	HER2	T2N0	IIA	-	Mucinous carcinoma

Clinicopathological parameters of 46 invasive breast cancer patients are shown followed by Table 2.

not caspase-9/3 and (iii) poor response: in MDA-MB-231 cells, Mieap activates apoptotic factors in the mitochondria (however, no caspases are activated, resulting in resistance to Mieap-induced cell death).

Second, Mieap protein was downregulated in tumors with more aggressive and malignant phenotypes of human breast cancer. In FA, which consists of both glandular breast tissue and stromal tissue, Mieap was expressed in the cytoplasm of glandular tissue in 16/18 (88.9%) cases. Interestingly, Mieap expression tended to decrease with malignant transformation (DCIS; 15/27 [55.6%], IDC; 24/75 [32%]; Table 1). These data suggest that Mieap plays an important role in preventing the malignant transformation and/or progression of breast tumors. Given that Mieap is under the control of p53, it is understandable that benign glandular tissues might express Mieap to suppress malignant transformation.

Third, p53/Mieap-regulated MQC is genetically and epigenetically inactivated in tumors with more aggressive and malignant human breast cancer phenotypes. The p53/Mieap/BNIP3-regulated MQC pathway is inactivated in >70% of colorectal cancers, suggesting that Mieap-regulated MQC has a critical role in colorectal cancer suppression in vivo.<sup>23</sup> In this study, we found that this pathway was inactivated in 12/46 (26.1%) invasive breast cancers via the promoter methylation of *Mieap* or p53 mutations, which occurred at a lower frequency compared to that observed for colorectal cancer. This might be due to the BNIP3 status in breast cancer. The promoter methylation of *BNIP3* was not detected in any breast cancer samples, whereas it occurred in nearly 50% colorectal cancer specimens. Interestingly, among 12 cases exhibiting inactivation of the pathway, 6 cases with methylation of the *Mieap* promoter were luminal B type, which comprises aggressive and fast-growing estrogen receptor-positive breast cancers. The other 6 cases with a p53 mutation were also aggressive types (triple negative, 4; HER2-rich, 1; luminal B, 1).<sup>30,31</sup> Furthermore, as shown in Table 2, there were 6 cases with p53 alterations, in which 5 were subjected to IHC for Mieap. Four of five cases did not express Mieap. Specifically, Mieap expression completely disappeared in 10 of 11 cases with either *Mieap* promoter methylation or p53 alterations. In contrast, only 1 expressed Mieap, despite

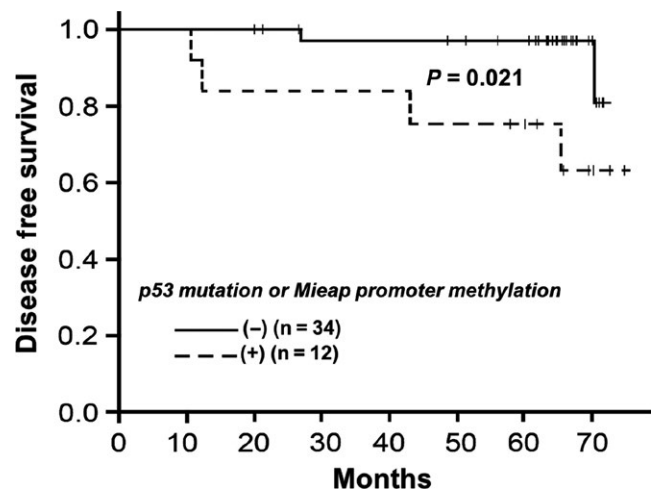


FIGURE 5 Kaplan-Meier curve showing disease-free survival (DFS) in breast cancer patients based on Mieap-regulated mitochondrial control (MQC) expression. The group with inactivated Mieap-regulated MQC (dotted line; n = 12) exhibited shorter DFS than that without genetic alterations (solid line; n = 34;  $P = 0.021$ )

the presence of a p53 mutation. This might be explained by the possibility that not only Mieap but some other p53-target genes are often induced in a p53-independent manner.

Fourth, the group with p53 mutation or *Mieap* promoter methylation showed shorter DFS, suggesting that inactivation of the p53/Mieap-regulated MQC pathway might lead to failed cell death induction, resulting in enhanced malignant potential and aggressiveness in vivo.

In summary, Mieap induces caspase-dependent apoptosis in breast cancer cells in vitro. Moreover, p53/Mieap-regulated MQC is inactivated in breast cancers with more aggressive and malignant phenotypes in vivo. Therefore, p53/Mieap-regulated MQC plays a critical role as a tumor suppressor in human breast cancer. Although there were limitations to our present work, this study forms the basis for future research projects to develop novel strategies to treat cancer.

## ACKNOWLEDGMENTS

We thank Shizu K for technical support and Enya K, Hirata M, Iwata A, Mori K and Takano K for administrative assistance.

## DISCLOSURE STATEMENT

KY has received grants and personal fees from Taiho Pharmaceutical, Pfizer, Chugai Pharmaceutical and Yakult Honsha, grants from Bristol-Myers Squibb and Kyowa Hakko Kirin, and honoraria from Taiho Pharmaceutical, Pfizer, Chugai Pharmaceutical, Kyowa Hakko Kirin and Yakult Honsha, and had a consultant and advisory relationship with Taiho Pharmaceutical and La Roche. All remaining authors declare that they have no conflict of interests.

## ORCID

Manabu Futamura  <http://orcid.org/0000-0001-5622-8352>

Hirofumi Arakawa  <http://orcid.org/0000-0001-6077-0638>

## REFERENCES

- International Agency for Research on Cancer. GLOBOCAN 2012: Estimated Cancer Incidence, Mortality and Prevalence Worldwide in 2012. <http://globocan.iarc.fr/Default.aspx>. Accessed December, 2017.
- Torre LA, Bray F, Siegel RL, Ferlay J, Lortet-Tieulent J, Jemal A. Global cancer statistics, 2012. *CA Cancer J Clin*. 2015;65:87-108.
- Collaborative Group on Hormonal Factors in Breast Cancer. Breast cancer and breastfeeding: collaborative reanalysis of individual data from 47 epidemiological studies in 30 countries, including 50 302 women with breast cancer and 96 973 women without the disease. *Lancet*. 2002;360:187-195.
- American Cancer Society. *Breast Cancer Facts & Figures 2015-2016*. Atlanta: American Cancer Society; 2015. <https://www.cancer.org/research/cancer-facts-statistics/breast-cancer-facts-figures.html>
- Antoniou A, Pharoah PD, Narod S, et al. Average risks of breast and ovarian cancer associated with *BRCA1* or *BRCA2* mutations detected in case Series unselected for family history: a combined analysis of 22 studies. *Am J Hum Genet*. 2003;72:1117-1130.
- Hollstein M, Sidransky D, Vogelstein B, Harris CC. p53 mutations in human cancers. *Science*. 1991;253:49-53.
- Coles C, Condie A, Chetty U, Steel CM, Evans HJ, Prosser J. p53 mutations in breast cancer. *Cancer Res*. 1992;52:5291-5298.
- Borresen-Dale AL. TP53 and breast cancer. *Hum Mutat*. 2003;21:292-300.
- The Cancer Genome Atlas Network. Comprehensive molecular portraits of human breast tumours. *Nature*. 2012;490:61-70.
- Yang P, Du CW, Kwan M, Liang SX, Zhang GJ. The impact of p53 in predicting clinical outcome of breast cancer patients with visceral metastasis. *Sci Rep*. 2013;3:2246.
- Vogelstein B, Lane D, Levine AJ. Surfing the p53 network. *Nature*. 2000;408:307-310.
- El-Deiry WS, Tokino T, Velculescu VE, et al. WAF1, a potential mediator of p53 tumor suppression. *Cell*. 1993;75:817-825.
- Oda K, Arakawa H, Tanaka T, et al. p53AIP1, a potential mediator of p53-dependent apoptosis, and its regulation by Ser-46-phosphorylated p53. *Cell*. 2000;102:849-862.
- Tanaka H, Arakawa H, Yamaguchi T, et al. A ribonucleotide reductase gene involved in a p53-dependent cell-cycle checkpoint for DNA damage. *Nature*. 2000;404:42-49.
- Futamura M, Kamino H, Miyamoto Y, et al. Possible role of semaphorin 3F, a candidate tumor suppressor gene at 3p21.3, in p53-regulated tumor angiogenesis suppression. *Cancer Res*. 2007;67:1451-1460.
- Nakamura Y, Arakawa H. Discovery of Mieap-regulated mitochondrial quality control as a new function of tumor suppressor p53. *Cancer Sci*. 2017;108:809-817.
- Arakawa H. p53, apoptosis and axon-guidance molecules. *Cell Death Differ*. 2005;12:1057-1065.
- Susan E. Apoptosis: A review of programmed cell death. *Toxicol Pathol*. 2007;35:495-516.
- Miyamoto Y, Kitamura N, Nakamura Y, et al. Possible existence of lysosome-like organelle within mitochondria and its role in mitochondrial quality control. *PLoS ONE*. 2011;6:e16054.
- Kitamura N, Nakamura Y, Miyamoto Y, et al. Mieap, a p53-inducible protein, controls mitochondrial quality by repairing or eliminating unhealthy mitochondria. *PLoS ONE*. 2011;6:e16060.
- Nakamura Y, Kitamura N, Shinogi D, et al. BNIP3 and NIX mediate Mieap-induced accumulation of lysosomal proteins within mitochondria. *PLoS ONE*. 2012;7:e30767.
- Tsuneki M, Nakamura Y, Kinjo T, Nakanishi R, Arakawa H. Mieap suppresses murine intestinal tumor via its mitochondrial quality control. *Sci Rep*. 2015;5:12472.
- Kamino H, Nakamura Y, Tsuneki M, et al. Mieap-regulated mitochondrial quality control is frequently inactivated in human colorectal cancer. *Oncogenesis*. 2016;4:e181.
- Zhang J, Ney PA. Role of BNIP3 and NIX in cell death, autophagy, and mitophagy. *Cell Death Differ*. 2009;16:939.
- Ohnishi S, Futamura M, Kamino H, et al. Identification of NEEP21, encoding neuron-enriched endosomal protein of 21 kDa, as a transcriptional target of tumor suppressor p53. *Int J Oncol*. 2010;37:1133-1141.
- Lakhani SA, Masud A, Kuida K, et al. Caspases 3 and 7: key mediators of mitochondrial events of apoptosis. *Science*. 2006;311:847-851.
- Zang SH, Huang Q. Etoposide induces apoptosis via the mitochondrial- and caspase-dependent pathways and in non-cancer stem cells in Panc-1 pancreatic cancer cells. *Oncol Rep*. 2013;30:2765-2770.
- Janicke RU, Sprengart ML, Wati MR, Porter AG. Caspase-3 is required for DNA fragmentation and morphological changes associated with apoptosis. *J Biol Chem* 1998;273:9357-9360.
- Oliver FJ, de la Rubia G, Rolli V, Ruiz-Ruiz MC, de Murcia G, Murcia JM. Importance of poly (ADP-ribose) polymerase and its cleavage in apoptosis. *J Biol Chem*. 1998;273:33533-33539.
- Goldhirsch A, Winer EP, Coates AS, et al. Personalizing the treatment of women with early breast cancer: highlights of the St Gallen International Expert Consensus on the Primary Therapy of Early Breast Cancer 2013. *Ann Oncol*. 2013;24:2206-2223.
- Hennigs A, Riedel F, Gondos A, et al. Prognosis of breast cancer molecular subtypes in routine clinical care: A large prospective cohort study. *BMC Cancer*. 2016;16:734.

## SUPPORTING INFORMATION

Additional supporting information may be found online in the Supporting Information section at the end of the article.

**How to cite this article:** Gaowa S, Futamura M, Tsuneki M, et al. Possible role of p53/Mieap-regulated mitochondrial quality control as a tumor suppressor in human breast cancer. *Cancer Sci*. 2018;109:3910-3920. <https://doi.org/10.1111/cas.13824>